(33) Olson, W. K. *Nucleic Acids Res.* **1975**, *2*, 2055–2068.
(34) Yathindra, N.; Sundaralingam, M. *Proc. Natl. Acad. Sci. U.S.A.* **1974**, *71*, 3325–3329.
(35) Prusiner, P.; Brennan, T.; Sundaralingam, M. *Biochemistry* **1973**, *12*, 1196–1202.
(36) Prusiner, P.; Sundaralingam, M. *Acta Crystallogr., Sect. B* **1976**, *32*, 419–426.
(37) Rohrer, D. C.; Sundaralingam, M. *J. Am. Chem. Soc.* **1970**, *92*, 4956–4962.
(38) Parthasarathy, R.; Davis, R. E. *Acta Crystallogr.* **1967**, *23*, 1049–1057.
(39) Singh, P.; Hodgson, D. J. *Biochemistry* **1974**, *13*, 5445–5452.
(40) Prusiner, P.; Sundaralingam, M. *Acta Crystallogr., Sect. B* **1978**, *34*, 517–523.
(41) Hutcheon, W. L.; James, M. N. G. *Acta Crystallogr., Sect. B* **1977**, *33*, 2224–2228.
(42) Sprang, S.; Scheller, R.; Rohrer, D.; Sundaralingam, M. *J. Am. Chem. Soc.* **1978**, *100*, 2867–2872.
(43) Sprang, S.; Sundaralingam, M. *Acta Crystallogr., Sect. B* **1973**, *29*, 1910–1916.
(44) Srikrishnan, T.; Parthasarathy, R. *Nature (London)* **1976**, *264*, 379–380.
(45) Young, P. R.; Kallenbach, N. R. *J. Mol. Biol.* **1978**, *126*, 467–479.
(46) Brahms, J.; Sadron, C. *Nature (London)* **1966**, *212*, 1309–1312.
(47) Ts'o, P. O. P. "Fine Structure of Proteins and Nucleic Acids", Sheff, Fasman and Tima, Eds.; Marcel Dekker: New York, 1970; pp 49–190.
(48) Spencer, M.; Fuller, W.; Wilkins, M. H. F.; Brown, G. L. *Nature (London)* **1962**, *194*, 1014–1020. Abraham, D. J. *J. Theor. Biol.* **1971**, *30*, 83–91. Rabczenko, A.; Shugar, D. *Acta Biochim. Pol.* **1971**, *18*, 387–402. **1972**, *19*, 89–91.
(49) Bolton, P. H.; Kearns, D. R. *Biochim. Biophys. Acta* **1978**, *517*, 329–337. *J. Am. Chem. Soc.* **1978**, *100*, 479–484.
(50) Jack, A.; Ladner, J. E.; Klug, A. *J. Mol. Biol.* **1976**, *108*, 619–649. Stout, D.; Mizuno, H.; Rao, S. T.; Swaminathan, P.; Rubin, J.; Brennan, T.; Sundaralingam, M. *Acta Crystallogr., Sect. B* **1978**, *34*, 1529–1544.
(51) Frey, C. M.; Stuehr, J. "Metal Ions in Biological Systems", Vol. I; Siegel, H., Ed.; Marcel Dekker: New York, 1974; pp 52–116.
(52) Sternglanz, H.; Subramanian, E.; Lacey, J. C. Jr.; Bugg, C. E. *Biochemistry* **1976**, *15*, 4797–4802.
(53) Fischer, B. E.; Bau, R. *J. Chem. Soc., Chem. Commun.* **1977**, 272–273.
(54) Louie, S.; Bau, R. *J. Am. Chem. Soc.* **1977**, *99*, 3874–3876.
(55) Bugg, C. E.; Marsh, R. E. *J. Mol. Biol.* **1967**, *25*, 67–82.
(56) Sundaralingam, M. *Acta Crystallogr.* **1966**, *21*, 495–506.
(57) (a) Viswamitra, M. A.; Swaminatha Reddy, B.; James, M.N.G., Williams, G. J. B. *Acta Crystallogr., Sect. B* **1972**, *28*, 1108–1116.
(57) (b) Viswamitra, M. A.; Swaminatha Reddy, B.; Hung-Yin Lin, G.; Sundaralingam, M. *J. Am. Chem. Soc.*, **1971**, *93*, 4565–4573.
(58) Saenger, W.; Suck, D.; Eckstein, F. *Eur. J. Biochem.* **1974**, *46*, 559–567.
(59) Hecht, S. M.; Sundaralingam, M. *J. Am. Chem. Soc.* **1972**, *94*, 4314–4319.
(60) Kraut, J.; Jensen, L. H. *Acta Crystallogr.* **1963**, *16*, 79–88.
(61) Neidle, S.; Kühlbrandt, W.; Achari, A. *Acta Crystallogy., Sect. B* **1976**, *32*, 1850–1855.
(62) Sundaralingam, M. *Biopolymers* **1969**, *7*, 821–860.
(63) Yoo, C. S.; Blank, G.; Pletcher, J.; Sax, M. *Acta Crystallogr., Sect B* **1974**, *30*, 1983–1987.
(64) Fujiwara, T. *Bull. Chem. Soc. Jpn.* **1973**, *46*, 863–871.
(65) Furberg, S. *Acta Chem. Scand.* **1955**, *9*, 1557–1566. Neutron diffraction of phosphoric acid has been carried out, but the full details have not been published: Cole, F. E.; Peterson, S. W. "Abstracts", American Crystallographic Association Meeting, Bozeman, Mont. 1964; p 66.
(66) Swaminathan, V.; Sundaralingam, M. *CRC Crit. Rev. Biochem.*, in press.

Dynamics of Nonadiabatic Atom Transfer in Biological Systems. Carbon Monoxide Binding to Hemoglobin

Joshua Jortner*[1a] and Jens Ulstrup[1b]

Contribution from the Department of Chemistry, Tel-Aviv University, Tel Aviv, Israel, and the Chemistry Department A, Building 207, The Technical University of Denmark, 2800 Lyngby, Denmark. *Received December 6, 1978*

Abstract: In this paper we advance a theory of nonadiabatic molecular group transfer processes in biological systems, which can be described in terms of a radiationless transition between vibronic levels corresponding to two distinct electronic configurations. The resulting multiphonon rate expression exhibits a continuous variation from a temperature-independent nuclear tunnelling rate at low temperatures to an activated rate at high temperatures. The theory is applied for the study of the recombination reaction between CO and hemoglobin (CO/Hb) in the temperature range 2–100 K. This process is accompanied by an electronic spin change of the system, is induced by weak second-order spin-orbit coupling, and involves large nuclear changes, whereupon the nonadiabatic multiphonon treatment is applicable. The CO/Hb recombination rate is expressed in terms of a product of a second-order spin-orbit electronic coupling term and a thermally averaged nuclear Franck-Condon vibrational overlap term. The experimental temperature dependence of the CO/Hb recombination can adequately be accounted for in terms of our theory, provided that the shift in the iron equilibrium configuration between the "free" and "bound" states is 0.4–0.5 Å, the characteristic frequency of the motion of the iron, coupled to the deformation mode of the heme group is $\sim$100 cm^{-1}, the upper limit for the energy change involved in the exoergic process is ~ -0.05 to -0.1 eV, and the second-order spin-orbit coupling term is 0.1–1 cm^{-1}. These nuclear and electronic parameters concur with the available information concerning structural and spectroscopic data for hemoglobin and related compounds.

I. Introduction

Electron transfer (ET) and atom or molecule transfer (AT) reactions play a central role in a variety of biological systems. Consecutive ET reactions represent the key steps in the primary events of photosynthesis[2,3] and in the respiratory chain.[4] Proton transfer is one of the most important elementary steps in the action of hydrolytic enzymes[5,6] and in the primary photochemical processes in some visual pigments.[7] Ligand substitution, i.e., the transfer of heavy molecular groups, is important in the binding of substrate molecules to the metal centers in hydrolytic metalloenzymes.[8,9] The transfer of heavy molecular groups is also the dominant elementary process in the reversible uptake of dioxygen, carbon monoxide, and other small molecules by myoglobin (Mb), hemoglobin (Hb), and related compounds.[10] In terms of general methodology several of these processes (e.g., ET in bacterial photosynthesis,[2a] proton translocation in excited rhodopsin,[2b] and the recombination of CO with Mb or Hb[10]) may be viewed as unimolecular processes in a biological supermolecule, which are expected to exhibit an Arrhenius-type temperature dependence. However, as originally pointed out by Longuet-Higgins and Higgs,[11] in contrast to the predictions of this law, the rate constant is not expected to vanish for $T \rightarrow 0$ owing to zero-point energy effects. In modern terminology this would be restated as tunnelling of molecular groups prevailing for $T \rightarrow 0$ and resulting in a temperature-independent unimolecular rate constant at low temperatures.

During the last decade the dynamics of some elementary biological processes were investigated over a broad temperature range from cryogenic temperatures around 2 K up to room

0002-7863/79/1501-3744$01.00/0

temperature. Notable examples are the light-induced oxidation of cytochrome *c* in the photosynthetic bacterium *Chromatium*,[2a,4] the recombination of CO and other small ligand molecules produced via photodissociation of its complex with β-Hb subunits with its parent deoxy form,[10] and the production of prelumirhodopsin from electronically exited rhodopsin.[7] In all these cases the unimolecular rate is found to be finite and nearly temperature independent at low temperatures, while the rate changes within a narrow temperature interval into an Arrhenius temperature dependence, characterized by a finite activation energy.

The classification of these biological reactions as unimolecular processes which exhibit pronounced effects of nuclear tunnelling at low temperature is, however, too general. To proceed with the formulation of a microscopic theory for such processes two classes of reactions must be distinguished: (1) adiabatic processes which proceed on a single potential energy surface (Typical examples would be most AT processes involving the transfer of heavy molecular groups (ligand substitution, inner sphere ET) and probably also many proton transfer reactions.); (2) nonadiabatic processes involving a transition between two zero-order potential surfaces which correspond to two distinct zero-order electronic configurations. A necessary condition for the nonadiabatic limit is the smallness of the residual electronic coupling matrix element which couples the zero-order states. Recent theoretical analysis[12-14] has shown that this limit prevails for ET in the cytochrome *c*–bacteriochlorophyll system in bacterial photosynthesis.

The theory of ET in biological systems as nonadiabatic multiphonon processes is now well developed.[13-16] It is isomorphous with the general quantum mechanical theory of homogeneous and heterogeneous ET processes, with the nonadiabatic rate constant being expressed as a product of a square of a two-center one-electron exchange integral and a thermally averaged Franck-Condon vibrational nuclear overlap integral. This nuclear contribution represents a "horizontal" transition between two nuclear potential surfaces (in contrast to the "vertical" transitions in spectroscopy) and results in a temperature-independent ET rate at low temperature, which passes into an Arrhenius equation at higher temperatures. This is in accord with the experimental data of De Vault and Chance for ET in *Chromatium*.[2a] On the other hand, the theoretical framework for the description of the more complicated AT processes[16-19] is far less comprehensive. Analysis of experimental data commonly rests on the interpretation of the low-temperature *T*-independent rates on the basis of the Gamov tunnelling formula.[7,10] This empirical approach requires further justification, as the Gamov formula was derived for the decay of a bound state into a continuum and is therefore not straightaway applicable to AT between manifolds of bound states.

In the present work we shall adopt the formalism of multiphonon electronic transitions to nonadiabatic AT reactions in biological systems. We shall establish the relation between nonadiabatic ET and AT processes and also show that the nuclear Franck-Condon vibrational overlap factors can be represented in a form akin to the Gamov formula. More specifically, we shall apply the theory to the interesting problem of the low-temperature recombination of CO with Hb.[10] Thus, rather than dwelling on general quantum mechanical treatments of model systems for multiphonon processes, we shall now proceed to formulate the theory of AT processes with special reference to this interesting system.

II. CO–Hb and CO–Mb Recombination Reactions

The recombination of CO with both subunits of Hb, derivatives of this compound, and protoheme, with CO being formed by photodissociation of the appropriate CO complexes, has been studied over the temperature interval 2–300 K.[10] From

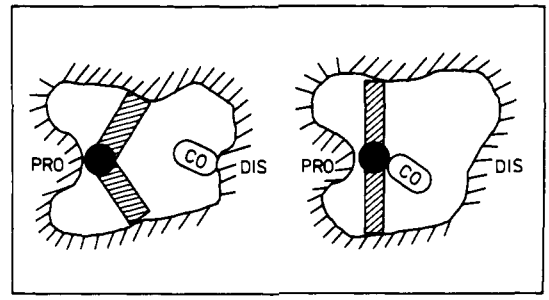

Figure 1. Schematic view of the Hb–CO recombination process. The heme group is seen from the edge and located in the hydrophobic pocket. The "proximal" and "distal" histidine are also indicated. The figure to the left corresponds to the initial state and the figure to the right to the final state.

previous studies of the recombination of CO with Mb it was shown that at temperatures below 180 K the system overcomes a single barrier corresponding to a shift in the CO position.[10a] At these low temperatures, the hydrophobic pocket which surrounds the heme group is sealed off, i.e., CO does not leave the pocket. In the initial "free" state CO is likely to be attached to the "distal" histidine in the protein chain lining the pocket, whereas it is bound to Fe^{2+} in the final state. Since this elementary process is the only one observed at low temperatures ($T < 180$ K), it is reasonable to assume that it is also the only one occurring in the CO–Hb recombination in the temperature range 2–100 K. The detailed experimental study of this process has provided the following information: (a) The rebinding process does not show an exponential decay but rather follows a power law. Nonexponential kinetics are characteristic of a unimolecular process subject to "inhomogeneous broadening". In the present case this effect originates from the energetic spread of the barrier heights due to the freezing of different conformational states. (b) The average half-times (or rather $\tau_{0.75}$, which refer to the time when the deoxy-Hb concentration has dropped to 75% of its initial value) is practically temperature independent in the range 2–10 K. (c) The transition from the tunnelling region (2–10 K) to the temperature-activated region occurs in the range 10–20 K. Above this region $\tau_{0.75}^{-1}$ is temperature dependent, characterized by an apparent activation energy of 0.045 eV.

We shall next consider the nuclear configurational changes and the electronic states involved in the recombination process. Crystallographic data suggested that in the CO-free five-coordinated state the iron atom is located 0.75 Å out of the puckered heme plane.[20] This value has been questioned by more recent data, which suggest a displacement similar to that for CO-free Mb.[21] The distance of the iron atom from the mean of the heme plane in this compound has been reported to be about 0.3 Å,[22,23] although recent data suggest the somewhat larger value of 0.55 Å[24] which is also found in certain model compounds.[25] In view of this discrepancy of reported values we shall prefer to leave this nuclear displacement of the iron atom as a parameter which will subsequently be estimated from the experimental kinetic data. In the bound CO–Hb state the iron atom is shifted into the heme plane (being only 0.02 Å out of the plane toward CO in model compounds[26]), while the CO molecule moves, probably from the "distal" histidine, to its bound state at the iron atom (Figure 1). The geometry of this bond is not known with certainty for the Hb–CO complex, but structural data[26a] show that for the Mb–CO complex the Fe–C–O angle is 135°, while for some related model compounds the Fe–C–O unit is linear.[26b]

Finally, we consider the relevant electronic states. The CO-free five-coordinated heme group is in the high-spin state ($S = 2$), while the heme group is in the low-spin state ($S = 0$) in the bound Hb–CO and Mb–CO complexes.[27] This is also

supported by recent theoretical calculations which provide strong evidence that the ground state of both complexes does correspond to the (Fe(S = 0) + CO(S = 0)) S = 0 state.[28a] In our treatment we shall consider just two electronic states, the "free" S = 2 state with the Fe outside the heme plane and the "bound" S = 0 state with the Fe within the heme plane. The location of the S = 1 state at different nuclear configurations is at present unknown. The calculations of Gouterman and colleagues[28b] indicate that for the planar configuration of the "free" Fe-porphine the S = 1 state is stable. However, recent spectroscopic studies[28c] indicate that the S = 1 state is located at high energies and should not be considered in relation to the dynamics of the recombination process.

The central features of the low-temperature CO-Hb and CO-Mb recombination processes which form the basis for our nonadiabatic AT theory are then the following: (A) The process involves a change in the electronic state of the system from S = 2 in the "free" state to S = 0 in the bound state. (B) The change in electronic state is accompanied by an appreciable change in the equilibrium nuclear configuration of the system.

III. Nonadiabatic AT Theory

Our approach toward a theory of nonadiabatic AT processes will now be specified as follows.

(1) The entire electronic-nuclear system can be adequately characterized by two distinct zero-order electronic states.

(2) For each of these electronic states we can construct a multidimensional Born-Oppenheimer potential surface determined by the nuclear displacements of the entire system.

(3) Two sets of vibronic levels for the nuclear potential surfaces can subsequently be found. These two sets constitute the quantum mechanical initial and final (zero-order) states of the system.

(4) A microscopic rate constant is derived by considering the system to be initially present in a vibronic level on the initial potential surface. Residual interactions which were not incorporated in the zero-order Hamiltonians couple the initial vibronic level to a manifold of vibronic levels belonging to the final potential surface, and which are quasi-degenerate with the initial vibronic level. Consequently, the initial vibronic level is metastable and undergoes a decay process. When the manifold of final state levels is dense, which is the case for solid-state systems such as the Hb-CO or Mb-CO systems, the decay is irreversible.

(5) Provided that the residual coupling which induces the process is weak relative to the characteristic vibrational frequencies, all the microscopic decay processes can be described in terms of time-dependent perturbation theory. This is the basic feature of the nonadiabatic description of the rate process, where the residual coupling is sufficiently low that the zero-order potential surfaces and the vibronic levels do not lose their identity.

(6) The time-dependent perturbation theory results in microscopic rate constants determined by Franck-Condon nuclear vibrational overlap integrals which can be handled by the theory of multiphonon processes.

(7) The macroscopic nonadiabatic rate is finally expressed in terms of a thermal average of the microscopic rates, the Gibbs averaging being taken over the manifold of initial vibronic levels.

The nonadiabatic AT process is thus essentially viewed as a nonradiative multiphonon process analogous to a variety of other nonadiabatic processes in solid-state physics, molecular physics, and solution chemistry including nonadiabatic ET.[13,29-32]

We now turn to the quantum mechanical formulation of the nonadiabatic AT problem. The Hamiltonian, H, of the entire system is

$$H(\mathbf{r},\mathbf{q}) = T(\mathbf{q}) + H_0(\mathbf{r},\mathbf{q}) + H_{SO}(\mathbf{r},\mathbf{q}) \quad (1)$$

where T is the nuclear kinetic energy, H_0 is the total electronic Hamiltonian at a fixed nuclear configuration, and H_{SO} is the spin-orbit coupling operator which has to be incorporated, since we shall be concerned with coupling between different spin states. $\mathbf{r}$ represents the collection of all electronic coordinates, while $\mathbf{q}$ denotes the collection of all the nuclear coordinates. Following the procedure generally applied in the theory of nonradiative processes in a dense medium we now separate the electronic and the nuclear motion defining Born-Oppenheimer electronic states, $\phi_I(\mathbf{r},\mathbf{q})$, which are eigenfunctions of $H_0(\mathbf{r},\mathbf{q})$, i.e.

$$H_0\phi_I(\mathbf{r},\mathbf{q}) = \epsilon_I(\mathbf{q})\phi_I(\mathbf{r},\mathbf{q}) \quad (2)$$

$\phi_I(\mathbf{r},\mathbf{q})$ (I = 1, 2, . . .) represents an orthonormal set of electronic wave functions, and $\epsilon_I(\mathbf{q})$ the corresponding nuclear potential surfaces. For the sake of simplicity we shall moreover limit ourselves to consideration of the two lowest electronic states of the CO-Hb system, which will be denoted by $\phi_a(\mathbf{r},\mathbf{q})$ (representing the high-spin state of the "free" Hb + CO) and $\phi_b(\mathbf{r},\mathbf{q})$ (corresponding to the low-spin state of iron bound to CO). The corresponding Born-Oppenheimer nuclear potential surfaces are thus $\epsilon_a(\mathbf{q})$ and $\epsilon_b(\mathbf{q})$, respectively, while the energies of all other electronic states are considered to be sufficiently high to give only perturbative contributions. As we are concerned with the dynamics of the two-electronic level system we shall subsequently expand the total time-dependent wave function as

$$\Psi(\mathbf{r},\mathbf{q},t) = \sum_{\alpha=a,b} \chi_\alpha(q,t)\phi_\alpha(\mathbf{r},\mathbf{q}) \quad (3)$$

where $\chi_\alpha(\mathbf{q},t)$ is a set of coefficients to be determined subsequently. Inserting this in the time-dependent Schrödinger equation, multiplying from the left with ϕ_β, and integrating with respect to the electronic coordinates we then obtain

$$\sum_{\alpha=a,b} \langle\phi_\beta|\hat{T} + \epsilon_\alpha(\mathbf{q}) + H_{SO} - ih\,\partial/\partial t|\chi_\alpha\phi_\alpha\rangle = 0;\ \beta = a, b \quad (4)$$

where $\langle\ \rangle$ denotes integration with respect to the electronic coordinates $\mathbf{r}$.

Introducing the nuclear kinetic energy operator, $\hat{T}$, as

$$\langle\phi_\beta|\hat{T}|\chi_\alpha\phi_\alpha\rangle = \hat{T}\chi_\alpha\delta_{\alpha\beta} + \langle\phi_\beta|\hat{L}|\phi_\alpha\rangle\chi_\alpha \quad (5)$$

where

$$\hat{L}|\phi_\alpha\rangle = \partial^2\phi_\alpha/\partial\mathbf{q}^2 + 2(\partial\phi_\alpha/\partial\mathbf{q})\partial/\partial\mathbf{q} \quad (6)$$

we get the coupled equations

$$[\hat{T} + \epsilon_\beta(\mathbf{q}) + \langle\phi_\beta|\hat{L} + H_{SO}|\phi_\beta\rangle - ih\partial/\partial t]\chi_\beta(\mathbf{q},t) = -\langle\phi_\beta|\hat{L} + H_{SO}|\phi_\alpha\rangle\chi_\alpha(\mathbf{q},t) \quad (7)$$

and a similar equation in which α and β are inverted. The perturbation terms which couple the pure spin states on the right-hand side of eq 7 thus involve nuclear kinetic energy terms reflecting the breakdown of the Born-Oppenheimer separability as well as spin-orbit interaction.

We complete the formal scheme by introducing the two sets of zero-order vibrational wave functions $\{\chi^0_{av}(\mathbf{q})\}$ for the potential surface $\epsilon_a(\mathbf{q})$ and $\{\chi^0_{bw}(\mathbf{q})\}$ for the surface $\epsilon_b(\mathbf{q})$. Within the Born-Oppenheimer scheme they are obtained from the equations

$$[\hat{T} + \epsilon_a(\mathbf{q}) + \langle\phi_\alpha|\hat{L} + H_{SO}|\phi_a\rangle - E^0_{av}]\chi^0_{av}(\mathbf{q}) = 0 \quad (8)$$

$$[\hat{T} + \epsilon_b(\mathbf{q}) + \langle\phi_b|\hat{L} + H_{SO}|\phi_b\rangle - E^0_{bw}]\chi^0_{bw}(\mathbf{q}) = 0 \quad (9)$$

where E^0_{bv} and E^0_{bw} are the energies of these vibronic levels.

We can now adopt Holstein's treatment of the mobility of small polarons, expanding the time-dependent coefficients $\chi_a(\mathbf{q},t)$ and $\chi_b(\mathbf{q},t)$ in terms of the complete basis sets $\{\chi^0_{av}(\mathbf{q})\}$ and $\{\chi^0_{bw}(\mathbf{q})\}$ in the nuclear space[33]

$$\chi_a(\mathbf{q},t) = \sum_v C_{av}(t)\chi^0_{av}(\mathbf{q}) \exp(-iE^0_{av}t/\hbar) \quad (10)$$

$$\chi_b(\mathbf{q},t) = \sum_w C_{bw}(t)\chi^0_{bw}(\mathbf{q}) \exp(-iE^0_{bw}t/\hbar) \quad (11)$$

The expansion coefficients then obey the equations of motion

$$ih\partial C_{av}/\partial t = -\sum_w C_{bw}\langle\phi_a|\hat{L} + H_{SO}|\phi_b\rangle \exp[-i(E^0_{bw} - E^0_{av})t/\hbar] \quad (12)$$

$$ih\partial C_{bw}/\partial t = -\sum_v C_{av}\langle\phi_b|\hat{L} + H_{SO}|\phi_a\rangle \exp[-i(E^0_{av} - E^0_{bw})t/\hbar] \quad (13)$$

We are now interested in the microscopic rate constant for the decay of a single vibronic level in the a manifold, i.e., $|av\rangle \rightarrow \{|bw\rangle\}$. The initial conditions are then $C_{av}(t=0) = 1$, while $C_{av'}(t=0) = 0$ for $v' \neq v$ and $C_{bw}(t=0) = 0$ for all w. Provided that the perturbation $\langle\phi_a|\hat{L} + H_{SO}|\phi_b\rangle$ is weak we can apply time-dependent perturbation theory for the solution of eq 12 and 13. The microscopic rate is then

$$W_{av} = \frac{2\pi}{\hbar}\sum_w |(\langle\phi_a(\mathbf{r},\mathbf{q})\chi^0_{av}(\mathbf{q})|\hat{R}| \times\phi_b(\mathbf{r},\mathbf{q})\chi^0_{bw}(\mathbf{q})\rangle)|^2\delta(E^0_{av} - E^0_{bw}) \quad (14)$$

where () denotes integration over the nuclear coordinates. $\hat{R}$ is the transition operator (the level shift operator[34]) which can be expanded in a perturbation series

$$R = (L + H_{SO}) + \sum_{c\neq a,b}\left\{\frac{(L + H_{SO})|\phi_c(\mathbf{r},\mathbf{q}_{0a})\rangle\langle\phi_a(\mathbf{r},\mathbf{q}_{0a})|(L + H_{SO})}{\epsilon_a(\mathbf{q}_{0a}) - \epsilon_c(\mathbf{q}_{0a})} + \frac{(L + H_{SO})|\phi_c(\mathbf{r},\mathbf{q}_{0b})\rangle\langle\phi_c(\mathbf{r},\mathbf{q}_{0b}|(L + H_{SO})}{\epsilon_b(\mathbf{q}_{0b}) - \epsilon_c(\mathbf{q}_{0b})}\right\} + \ldots \quad (15)$$

where the summation over all the electronic states c involves only the highly excited electronic configurations of the system. The electronic wave functions and potential energies of these c states can be taken with sufficient accuracy at the nuclear equilibrium configurations, $\mathbf{q}_{0a}$ and $\mathbf{q}_{0b}$ of the two lowest potential surfaces (crude adiabatic states[35]). The first term of $\hat{R}$ in eq 15 yields the Fermi golden rule. When this term identically vanishes, the second-order term acquires a special importance being the lowest term of finite value. Finally, the δ function in eq 14 ensures energy conservation. For real systems they serve rather as a "bookkeeping" device since the discrete levels are "broadened" by coupling to the medium. The δ function should thus in effect be replaced by a Lorentzian the width of which expresses the finite decay probability of the individual levels.[13]

In order to simplify the nonadiabatic rate constant given by eq 14 we shall invoke the Condon approximation separating the integrations over the nuclear and electronic coordinates. This procedure is expected to be adequate for the spin-orbit coupling since this operator is of electronic origin and therefore only weakly dependent on the nuclear coordinates. On the other hand, the Condon scheme requires some modifications for the L operator.[36] Since, however, we shall be interested primarily in the spin-orbit coupling we shall assume that the Condon scheme is adequate and write the microscopic rate as

$$W_{av} = \frac{2\pi}{\hbar}|V_{ab}|^2\sum_w |(\chi^0_{av}(\mathbf{q})|\chi^0_{bw}(\mathbf{q}))|^2\delta(E^0_{av} - E^0_{bw}) \quad (16)$$

where the electronic coupling term is

$$V_{ab} = \langle\phi_a|\hat{R}|\phi_b\rangle \quad (17)$$

When the first-order contribution to $\hat{R}$ is finite, then the electronic coupling is

$$V_{ab} = \langle\phi_a|\hat{L} + H_{SO}|\phi_b\rangle = \begin{cases}\langle\phi_a|\hat{L}|\phi_b\rangle & \text{case I}\\ \langle\phi_a|H_{SO}|\phi_b\rangle & \text{case II}\end{cases} \quad (18)$$

Case I prevails when ϕ_a and ϕ_b belong to the same states, and case II applies when they belong to different spin states. If the first-order contribution to eq 15 vanishes because of spin selection rules, or selection rules for spin-orbit coupling, the electronic coupling term in second order becomes

$$V_{ab} = \sum_{c\neq a,b}\left\{\frac{\langle\phi_a|\hat{L} + H_{SO}|\phi_c\rangle\langle\phi_c|\hat{L} + H_{SO}|\phi_b\rangle}{\epsilon_a(\mathbf{q}_{0a}) - \epsilon_c(\mathbf{q}_{0a})} + \frac{\langle\phi_a|\hat{L} + H_{SO}|\phi_c\rangle\langle\phi_c|\hat{L} + H_{SO}|\phi_b\rangle}{\epsilon_b(\mathbf{q}_{0b}) - \epsilon_c(\mathbf{q}_{0b})}\right\} \text{ case III} \quad (19)$$

V_{ab} in eq 16 thus incorporates direct spin-orbit coupling terms, second-order mixed spin-orbit-vibronic terms, and second-order vibronic contributions.

The microscopic rate constant for nonadiabatic AT, eq 16, is now expressed as products of an electronic coupling term, eq 18 or 19, and a Franck-Condon vibrational overlap factor. The microscopic rate constant is subsequently obtained as the thermally averaged probability for the process $\{|av\rangle\}_T \rightarrow \{|bv\rangle\}$, where $\{|av\rangle\}_T$ now denotes thermal averaging. The resulting macroscopic rate is then

$$W = \sum Z_{exp}^{-1}(-\beta E^0_{av}W_{av} = \frac{2\pi}{\hbar}|V_{ab}|^2 Z^{-1} \times\sum_v\sum_w \exp(-\beta E^0_{av})|(\chi^0_{av}|\chi^0_{bw})|^2\delta(E^0_{av} - E^0_{bw}) \quad (20)$$

where $Z = \Sigma_v \exp(-\beta E^0_{av})$ is the partition function for the initial manifold of vibrational states, and $\beta = (k_B T)^{-1}$. The macroscopic nonadiabatic rate constant is thus expressed as a product of the electronic coupling term and a thermally averaged Franck-Condon vibrational overlap integral, segregating the nuclear and the electronic contributions to the transition probability.

The question now arises whether the nonadiabatic approach, represented by eq 20, is in fact applicable to the low-temperature unimolecular recombination between CO and Hb. This requires that three basic conditions are satisfied. Firstly, regarding the electronic contribution, the process must involve a change in the electronic state of the system. We have already seen that this is indeed so, as the electronic states ϕ_a and ϕ_b correspond to $S = 2$ and $S = 0$ (zero order) pure spin states (section II, point A). The residual interaction which induces the coupling between the zero-order vibronic states now involves the spin-orbit interaction. Secondly, concerning the nuclear contribution, the Franck-Condon vibrational overlap factors have to be appreciable in order that the relaxation process is efficient. This is ensured by the nuclear geometrical rearrangement accompanying the process (section II, point B). Thirdly, the nonadiabatic limit must be applicable, which rests on the notion of "weak" coupling (small V_{ab}). We shall return to this point in section IV after the analysis of the experimental data for the CO-Hb system.

The theoretical treatment of the low-temperature CO-Hb recombination is now conceptually straightforward, although,

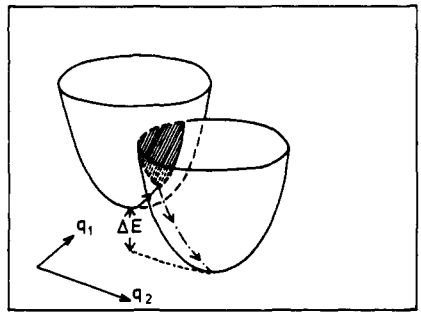

Figure 2. Three-dimensional potential surfaces spanned by the two coordinates q_1 and q_2. The two-dimensional interaction "surface", the saddle point of this surface, and a trajectory via this point are indicated.

as we shall see in section IV, this task is fraught with considerable technical difficulties. Before alluding to any, necessarily simplified, specific model for the electronic and nuclear contributions to the nonadiabatic AT rate, it is, however, appropriate to consider some general characteristics of the rate expression of eq 20.

1. The Low-Temperature Limit. At sufficiently low temperatures the level spacings between the lowest initial vibrational zero-order state E^0_{a0} ($v = 0$) and all other zero-order states in the initial manifold are much larger than the thermal energy, i.e.

$$|E^0_{av} - E^0_{a0}| \gg k_B T \tag{21}$$

The AT process then proceeds, from the lowest state $\phi_a \chi_{a0}$, and this is only possible if the AT process is exoergic, i.e.

$$\Delta E = E^0_{a0} - E^0_{b0} > 0 \tag{22}$$

The low-temperature rate constant is then W_{a0}, or more explicitly

$$W(T \to 0) = W_{a0} = \frac{2\pi}{\hbar} |V_{ab}|^2 \sum_w |(\chi^0_{a0}|\chi^0_{bw})^2 \delta(E^0_{a0} - E^0_{bw}) \tag{23}$$

The finite temperature-independent low-temperature rate is determined by the Franck–Condon vibrational overlap of χ^0_{a0} with all the χ_{bw} states which are isoenergetic with this state. Physically, this corresponds to temperature-independent nuclear tunnelling from the lowest zero-point energy state of the initial nuclear configuration to the final vibronic states which are nearly degenerate with this level.

2. The High-Temperature Limit. At sufficiently high temperatures the rate constant can be expressed in terms of the adiabatic potential surfaces $\epsilon_a(\mathbf{q})$ and $\epsilon_b(\mathbf{q})$ rather than the quantized vibronic levels.[37] For rather general forms of $\epsilon_a(\mathbf{q})$ and $\epsilon_b(\mathbf{q})$ the condition for this limit is equivalent to the variation of the potential energy in the initial state within the averaged De Broglie wavelength, $\hbar/(\mu k_B T)^{1/2}$ (where μ is a characteristic nuclear mass), being negligible compared with the thermal energy,[37] i.e.

$$[\hbar/(\mu k_B T)^{1/2} \partial/\partial q_j]^n \epsilon_a(\mathbf{q}) \ll k_B T \tag{24}$$

Exploiting the classical form of the Franck–Condon principle we can then write the transition probability, eq 20, in the semiclassical form

$$W = \frac{2\pi}{\hbar} Z_{cl}^{-1} |V_{ab}|^2 \int \exp[-\epsilon_a(\mathbf{q})/k_B T] \delta[\epsilon_b(\mathbf{q}) - \epsilon_a(\mathbf{q})] \tag{25}$$

with the classical partition function

$$Z_{cl} = \int d\mathbf{q} \exp[-\epsilon_a(\mathbf{q})/k_B T] \tag{26}$$

and the integrations carried out over all the nuclear coordinates, $\mathbf{q} = \{q_a \ldots q_N\}$ in the N-dimensional space. The occurrence of the δ function in eq 25 implies that the only nonvanishing contributions to the integral are provided by the intersection points of the potential surfaces (Figure 2) and the exponential function moreover means that the dominating contribution is proportional to $\exp[-\epsilon_a(\mathbf{q}_s)/k_B T]$, where $\mathbf{q}_s$ is the lowest point on the intersection surface. The high-temperature rate expression assumes an Arrhenius-type form with the activation energy being determined by $\epsilon_a(\mathbf{q}_s)$. For the particular case where the potential surfaces are characterized by a single coordinate q, and the surfaces intersect at the point q_s, the rate expression is

$$W = \frac{2\pi}{\hbar} Z^{-1} |V_{ab}|^2 \left| \frac{\partial}{\partial q} [\epsilon_b(q) - \epsilon_a(q)] \right|^{-1}_{q=q_s} \times \exp[-\epsilon_a(q_s)/k_B T] \tag{27}$$

This activated rate expression is derived without invoking the concept of an activated complex, since q_s is just a particular point on the initial state potential surface.[37,38]

In summary we emphasize that eq 23 and 25 are both limiting cases of the same general quantum mechanical rate expression, eq 20, which passes from a tunnelling rate constant at low temperature to an activated rate constant at high temperatures. The overall rate should therefore not be expressed as the sum of a tunnelling rate and a thermally activated rate.[10]

We shall conclude this section by comparing the rate equation for the nonadiabatic AT process, eq 20, with the corresponding result for nonadiabatic ET processes both in biological systems[13,14] and for homogeneous ET processes in general.[17-19,30,39,40] The important analogies involve several of the general features of multiphonon processes.

(1) Both nonadiabatic ET and AT rate constants are expressed as products of an electronic coupling term and a nuclear Franck–Condon factor.

(2) The nuclear Franck–Condon factor appears in the theory of both ET and AT processes, since both categories are viewed as transitions between nuclear states of the system.

(3) The temperature-independent tunnelling process manifested at low temperatures involves nuclear tunnelling both for ET and for AT.

(4) In both cases the high-temperature activated rate involves thermal activation to the lowest intersection point of the nuclear Born–Oppenheimer potential surfaces.

However, two qualitative differences between nonadiabatic AT of the kind considered in the present work and ET processes should be emphasized.

(5) The electronic coupling term, V_{ab}, for a nonadiabatic AT process involving the transfer of a heavy atom group (such as the CO–Hb recombination) is associated with spin–orbit interaction. The corresponding electronic coupling for ET involves a two-center one-electron exchange integral.

(6) The nature of the changes in the nuclear configurations which determine the Franck–Condon vibrational overlap factors is qualitatively different for ET and many AT processes. For ET the changes in the nuclear configuration of the entire system consisting of the electron donor, the electron acceptor, and the external medium can be separated into two groups. One group corresponds to the long-range coupling with the optical phonons of the outer medium which responds to the change in the charge distribution. For a variety of ET processes coupling to these polar modes give a dominating contribution to the activation energy. The early work of Marcus[39] and of Levich and Dogonadze[40] considered exclusively these long-range interactions. The second group involves coupling with high-frequency molecular vibrational modes of the electron donor and/or acceptor centers. This short-range coupling is

crucial in determining the characteristics of the nonadiabatic ET in *Chromatium*.[13,14] On the other hand, for AT processes involving the transfer of an electrically neutral group the nuclear configurational changes in the immediate vicinity of the reaction center are expected to be of primary importance, while the effects of long-range coupling are negligible. For the Hb-CO reaction these nuclear modes involve Fe-ligand bending and the motion of the CO molecule relative to the iron atom. In addition, short-range coupling to low-frequency acoustic phonon modes[41] may also be important for the AT process.

IV. Model Calculations for the Hb-CO System

In order to exploit the theory outlined above we shall have to characterize two sets of quantities, i.e., the electronic coupling, V_{ab}, which is determined by the nature of the electronic states involved in the process, and the Franck-Condon vibrational overlap factors, which can be evaluated from the appropriate structural information regarding the nuclear configurational changes and from spectroscopic information concerning the characteristic force constants for the molecular motion. In practice, a priori calculation of these quantities is prohibitively difficult by the lack of detailed information of both the electronic wave functions and the relevant vibrational spectroscopic data. In what follows we shall therefore consider some general features of the electronic coupling term and subsequently provide some simple model calculations for the nuclear contribution.

The electronic coupling term, V_{ab}, for the Hb-CO and Mb-CO recombination processes (eq 18 and 19) combines ϕ_a ($S = 2$) and ϕ_b ($S = 0$) zero-order pure spin states. It is immediately apparent that the first-order contribution of the nonadiabaticity operator $\hat{L}$ to eq 18 vanishes. Furthermore, as the spin-orbit coupling is a one-electron operator, it obeys the selection rule $\Delta S = \pm 1$,[42] so that $\langle \phi_a(S = 2)|H_{SO}|\phi_b(S = 0)\rangle = 0$. Thus, the first-order contribution to V_{ab}, eq 18, vanishes, and we must consider case III (eq 19). The nonvanishing perturbative contributions for the excited ϕ_c electronic states can originate only from ϕ_c ($S = 1$) states. Consequently, the operator L contributes neither to the coupling between ϕ_b ($S = 0$) and ϕ_c ($S = 1$) nor between ϕ_a ($S = 2$) and ϕ_c ($S = 1$). The resulting electronic coupling appropriate to the system is then the second-order spin-orbit coupling contribution

$$V_{ab} \approx \langle H_{SO}\rangle_{ac}\,\langle H_{SO}\rangle_{cb}/\Delta\epsilon$$

where $\langle H_{SO}\rangle_{\alpha\beta}$ are the integrals of spin-orbit coupling between the electronic states ϕ_α and ϕ_β ($\alpha, \beta = a, b, c$) and $\Delta\epsilon$ the energy gap between ϕ_a or ϕ_b and ϕ_c.

Typical values of spin-orbit coupling terms for first-row transition metal ions are $\langle H_{SO}\rangle_{\alpha\beta} \approx 100$ cm^{-1} [42,43] which together with $\Delta\epsilon \approx 10^4$ cm^{-1} give the crude estimate of $V_{ab} \approx 1$ cm^{-1} for the Hb-CO and Mb-CO systems. We notice here that such an analysis would be more involved for the Hb-O_2 recombination, as the Hb-O_2 complex, unlike the Hb-CO complex, is characterized by a large number of low-lying electronic states.[44,45]

Next we turn to a rough estimate of the nuclear vibrational overlap factors. In this context we have to consider vibrational modes exhibiting a large change in their equilibrium configuration when going from the CO-"free" to the bound state. Two such "intramolecular" modes have to be considered (Figure 2). Firstly, the motion of the iron atom can be considered as a metal-ligand bending mode coupled to deformational motion in the puckered heme plane. The corresponding frequency is unknown but frequencies in the range 150-200 cm^{-1} for simple heme complexes have been ascribed to this motion.[46] Also, force constants for this mode obtained from ab initio calculations on model compounds give frequency values in the range 100-150 cm^{-1} depending on the effective

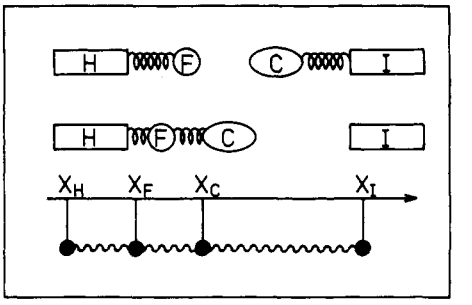

Figure 3. Simplified view of the four-atom group representation of the Hb-CO recombination process. The interaction between the various molecular fragments is indicated by the "springs" or the wiggly lines.

mass associated with the mode.[47] Moreover, as noted, the equilibrium configuration of this mode is shifted by 0.3-0.5 Å during the recombination process. Secondly, CO is initially weakly associated with the "distal" histidine, while it is bound to Fe in the final state. The configurational changes, if any, involved in the CO-histidine motion are unknown. To provide some intuitive feeling for the nature of the nuclear dynamics of the process we shall advance a grossly oversimplified model (Figure 3) for the nuclear motion consisting of a linear four-atom array H-F-C-I, where H is the five-coordinated heme site, F is the iron atom, C is CO, and I is the histidine group. Furthermore, we assume that the masses $m_H, m_I \gg m_C, m_F$ where the indexes indicate the appropriate molecular groups. The nuclear Hamiltonians in the initial and final states, h_a and h_b, are then

$$h_\alpha = T + \epsilon_\alpha(\mathbf{q}) \qquad \alpha = a,b \tag{28}$$

(cf. eq 8 and 9), for which we shall now provide explicit expressions.

Introducing the coordinates X_j of the various groups (j) in the linear array we can write generally

$$h_\alpha = -\frac{\hbar^2}{2}\sum_i \frac{1}{m_i}\partial^2/\partial X_i^2 + V^\alpha_{HF}(X_F - X_H) + V^\alpha_{FC}(X_C - X_F) + V^\alpha_{CI}(X_I - X_C) \tag{29}$$

where V_{ij} is the appropriate effective potentials of interaction between the groups. After separation of the center-of-mass motion the nuclear Hamiltonian is

$$h_\alpha = [-(\hbar^2/2\mu_{HF})\partial^2/\partial X_{HF}^2 + V_{HF}(X_{HF})] + [-(\hbar^2/2\mu_{CI})\partial^2/\partial X_{CI}^2 + V_{CI}(X_{CI})] + [-(\hbar^2/2\mu_{HF,CI})\partial^2/\partial X_{HF,CI}^2 + V^\alpha_{FC}(X_{HF,CI} - \gamma_{I,CI}X_{CI} - \gamma_{H,HF}X_{HF})] \tag{30}$$

where we have defined the following coordinates

$$X_{HF} = X_F - X_H;\ X_{CI} = X_I - X_C \tag{31}$$

$$X_{HF,CI} = (m_C X_C + m_I X_I)/(m_C + m_I) - (m_H X_H + m_F X_F)/(m_H + m_F) \tag{32}$$

which correspond to the internal distances in the HF and CI "fragments" and to the distances between the centers of mass of HF and CI. The reduced masses are

$$\mu_{HF} = m_H m_F/(m_H + m_F);\ \mu_{CI} = m_C m_I/(m_C + m_I) \tag{33}$$

$$\mu_{HF,CI} = (m_H + m_F)(m_C + m_I)/(m_H + m_F + m_C + m_I) \tag{34}$$

and the mass ratios

$$\gamma_{I,CI} = m_I/(m_C + m_I);\ \gamma_{H,HF} = m_H/(m_H + m_F) \tag{35}$$

in the limit of very large masses of H and I this becomes

$$X_{HF,CI} \approx X_I - X_H;\ \mu_{HF} \approx m_F;\ \mu_{CI} \approx m_C \tag{36}$$

$$\mu_{HF,Cl} \approx m_H m_l/(m_H + m_l) \text{ and } \gamma_{l,Cl} \approx \gamma_{H,HF} \approx 1 \quad (37)$$

At this stage we separate the interaction potential V^{α}_{FC} into an interaction between rigid HF and Cl units at their equilibrium configurations $\bar{X}^{\alpha}_{HF}$ and $\bar{X}^{\alpha}_{Cl}$ and a residual term. The Hamiltonian for the nuclear reaction is then $h_{\alpha} = h^0{}_{\alpha} + V_{\alpha}$, where the zero-order nuclear Hamiltonian, $j^0{}_{\alpha}$, is

$$\begin{aligned} h^0{}_{\alpha} = {} & [-\hbar^2/2\mu_{HF})\partial^2/\partial X_{HF}{}^2 + V^{\alpha}{}_{HF}(X_{HF})] \\ & + [-(\hbar^2/2\mu_{Cl})\partial^2/\partial X_{Cl}{}^2 + V^{\alpha}{}_{Cl}(X_{Cl})] \\ & + [-(\hbar^2/2\mu_{HF,Cl})\partial^2/2\partial X_{HF,Cl}{}^2 \\ & + V^{\alpha}{}_{FC}(X_{HF,Cl} - \bar{X}^{\alpha}{}_{HF} - X^{\alpha}{}_{Cl})] \end{aligned} \quad (38)$$

while the residual contribution, V_{α}, is

$$\begin{aligned} V_{\alpha} = {} & V^{\alpha}{}_{FC}(X_{HF,Cl} - X_{HF} - X_{Cl}) \\ & - V^{\alpha}{}_{FC}(X_{HF,Cl} - \bar{X}^{\alpha}{}_{HF} - \bar{X}^{\alpha}{}_{Cl}) \end{aligned} \quad (39)$$

We assume that the residual term, V_{α}, is small and can be disregarded in this preliminary analysis of the nuclear dynamics. The nuclear coordinates are then X_{HF}, X_{Cl}, and $X_{HF,Cl}$, and the nuclear Hamiltonian, eq 30 and 38, is separable in these coordinates giving three independent contributions. The nuclear eigenstates for the electronic configurations ϕ_a and ϕ_b can thus be written

$$\chi^0{}_{av}(\mathbf{q}) = f_{v_1}(X_{HF}) f_{v_2}(X_{Cl}) f_{v_3}(X_{HF,Cl}) \quad (40)$$

$$\chi^0{}_{bw}(\mathbf{q}) = g_{w_1}(X_{HF}) g_{w_2}(X_{Cl}) g_{w_3}(X_{HF,Cl}) \quad (41)$$

where the v's and w's are appropriate vibrational quantum numbers. The nuclear wave functions appearing in eq 40 and 41 are eigenfunctions of the following equation (cf. eq 38).

$$[-(\hbar^2/2\mu_{HF})\partial^2/\partial X_{HF}{}^2 + V^a{}_{HF}(X_{HF})] f_{v_1}(X_{HF}) = \epsilon^0{}_{v_1} f_{v_1}(X_{HF}) \quad (42)$$

$$[-(\hbar^2/2\mu_{HF})\partial^2/\partial X_{HF}{}^2 + V^b{}_{HF}(X_{HF})] g_{w_1}(X_{HF}) = \epsilon^0{}_{w_1} g_{w_1}(X_{HF}) \quad (43)$$

$$[-(\hbar^2/2\mu_{Cl})\partial^2/\partial X_{Cl}{}^2 + V^a{}_{Cl}(X_{Cl})] f_{v_2}(X_{Cl}) = \epsilon^0{}_{v_2} f_{v_2}(X_{Cl}) \quad (44)$$

$$[-(\hbar^2/2\mu_{Cl})\partial^2/\partial X_{Cl}{}^2 + V^b{}_{Cl}(X_{Cl})] g_{w_2}(X_{Cl}) = \epsilon^0{}_{w_2} g_{w_2}(X_{Cl}) \quad (45)$$

$$[-(\hbar^2/2\mu_{HF,Cl}) + V^a{}_{FC}(X_{HF,Cl} - \bar{X}^a{}_{HF} - \bar{X}^a{}_{Cl})] f_{v_3}(X_{HF,Cl}) = \epsilon^0{}_{v_3} f_{v_3}(X_{HF,Cl}) \quad (46)$$

$$[-(\hbar^2/2\mu_{HF,Cl}) + V^b{}_{FC}(X_{HF,Cl} - \bar{X}^b{}_{HF} - \bar{X}^b{}_{Cl})] g_{w_3}(X_{HF,Cl}) = \epsilon^0{}_{w_3} g_{w_3}(X_{HF,Cl}) \quad (47)$$

and the corresponding total energies of the vibronic states are $E^0{}_{bv} = \epsilon^0{}_{v_1} + \epsilon^0{}_{v_2} + \epsilon^0{}_{v_3}$ and $E^0{}_{bw} = \epsilon^0{}_{w_1} + \epsilon^0{}_{w_2} + \epsilon^0{}_{w_3}$. We notice here that, if we would go beyond the present crude approximation and incorporate the V_{α} term (eq 39), all we have to do is to form combinations of the basis sets, eq 40 and 41, of the form

$$\chi_{av} = \sum_{v_1 v_2 v_3} C_{v_1 v_2 v_3} f_{v_1} f_{v_2} f_{v_3} \quad (48)$$

$$\chi_{bw} = \sum_{w_1 w_2 w_3} C_{w_1 w_2 w_3} g_{w_1} g_{w_2} g_{w_3} \quad (49)$$

and to diagonalize the total Hamiltonian, eq 30. This extension is similar to incorporating configuration interaction effects in the theory of electronic structure. At present we shall, however, refrain from pursuing this.

Within the simple model outlined we have been able to represent the nuclear states of the Hb–CO reaction center as products of three "molecular" functions, eq 40–47. The heme–Fe motion is thus represented by f_{v_1} and g_{w_1}, the CO–histidine motion by f_{v_2} and g_{w_2}, and the relative motion of heme and histidine by f_{v_3} and g_{w_3}. The vibrational wave functions f_{v_1}, f_{v_2}, and f_{v_3} thus represent the initial Hb + CO state, while g_{w_1}, g_{w_2}, and g_{w_3} represent the final Hb–CO bound state. The Franck–Condon factors contained in the rate expression, eq 20, are then obtained in the factorized form

$$(\chi^0{}_{av}(q)|\chi^0{}_{bw}(q) = \eta_1(v_1,w_2)\eta_2(v_2,w_2)\eta_3(v_3,w_3) \quad (50)$$

where

$$\eta_1(v_1,w_1) = \int dX_{HF} f_{v_1}(X_{HF}) g_{w_1}(X_{HF}) \quad (51)$$

$$\eta_2(v_2,w_2) = \int dX_{Cl} f_{v_2} g_{w_2}(X_{Cl}) \quad (52)$$

$$\eta_3(v_3,w_3) = \int dX_{HF,Cl} f_{v_3}(X_{HF,Cl}) g_{w_3}(X_{HF,Cl}) \quad (53)$$

The introduction of the crude four-atom group model and the resulting single-bond nuclear states avoids the explicit use of the language of normal modes. This is convenient, as the AT process involves such large modification of the bonding that transformation of normal modes between the initial state and the final state would otherwise have to be involved. In addition, we also have to consider the role of low-frequency acoustic phonon modes. If some of these modes are subject to equilibrium coordinate shift during the process, they would have to be incorporated as accepting modes, but, as no direct information about this is available, we shall not do so. However, the low-frequency medium phonon modes are also expected to play a crucial role by inducing vibrational relaxation in the final state manifold $\{\chi^0{}_{bw}\}$. In the exoergic $\chi^0{}_{av} \rightarrow \{\chi^0{}_{bw}\}$ process this manifold is produced in highly vibrationally excited states, and the low-frequency medium modes induce fast vibrational relaxation subsequent to the electronic process, ensuring the irreversibility of the AT process. An analysis of this problem for small polaron motion, i.e., for a symmetrical nonadiabatic ET, was recently given by Holstein,[49] who concluded that incorporation of the consecutive vibrational relaxation process provides a justification for the rate equations of nonadiabatic processes involving a small number of molecular vibrations. With reference to eq 20 and 50 the quantum mechanical rate expression for the nonadiabatic AT process can then be written

$$\begin{aligned} W = {} & \frac{2\pi}{\hbar} Z^{-1} |V_{ab}|^2 \\ & \times \sum_{\substack{v_1 v_2 v_3 \\ w_1 w_2 w_3}} \exp[-(\epsilon^0{}_{v_1} + \epsilon^0{}_{v_2} + \epsilon^0{}_{v_3})/k_B T] |\eta_1(v_1,w_1)|^2 \\ & \times |\eta_2(v_2,w_2)|^2 |\eta_3(v_3,w_3)|^2 \delta(\epsilon^0{}_{v_1} - \epsilon^0{}_{w_1} + \epsilon^0{}_{v_2} \\ & - \epsilon^0{}_{w_2} + \epsilon^0{}_{v_3} - \epsilon^0{}_{w_3} - \Delta E) \end{aligned} \quad (54)$$

where it is understood that the low-frequency phonon modes act as "hidden variables" inducing vibrational relaxation subsequent to the electronic transition, ensuring the irreversibility of the process.

The three-bond equation can now be expressed in terms of a triple convolution of line-shape functions corresponding to the individual three molecular modes[30]

$$W = \frac{2\pi}{\hbar} |V_{ab}|^2 \int d\epsilon' \int d\epsilon'' F_1(\bar{E} - \epsilon') F_2(\epsilon' - \epsilon'') F_3(\epsilon'') \quad (55)$$

where

$$\bar{E} = (\epsilon^0{}_{v_1} + \epsilon^0{}_{v_2} + \epsilon^0{}_{v_3}) - (\epsilon^0{}_{w_1} + \epsilon^0{}_{w_2} + \epsilon^0{}_{w_3}) - \Delta E \quad (56)$$

$$F_1(X) = Z_I{}^{-1} \sum_{v_I} \sum_{w_I} |\eta_I(v_I,w_I)|^2 \delta(X) \quad I = 1, 2, 3 \quad (57)$$

$$Z_I = \sum_{v_I} \exp(-\epsilon^0{}_{v_I}/k_B T) \quad (58)$$

However, in view of the absence of structural and spectroscopic information, especially regarding the CO–histidine interaction, this equation is not very useful, and to obtain tractable results we are forced to introduce further simplifying assumptions, which can be relaxed when the appropriate information becomes available. Firstly, the relative motion of the groups HF and CI is characterized by a very low frequency due to the large reduced mass $\mu_{HF,CI}$. This low frequency motion which essentially mimics the medium modes is not likely to exhibit large configurational changes, and it is therefore reasonably incorporated with the other medium modes and its contribution to eq 55 disregarded. Secondly, in view of the lack of information about the CO–histidine motion (f_{v_2} and g_{w_2}) we shall also ignore the contributions of this mode to eq 55 and only consider the displacement of Fe relative to the heme plane. The omission of the contribution of the CO–histidine motion involves the most serious approximation inherent in the derivation of our final rate expression. This approximation is likely to be adequate in view of the presumably much larger nuclear displacement of the Fe–heme mode. The AT rate equation then simplifies to

$$W = \frac{2\pi}{\hbar} Z_1^{-1} |V_{ab}|^2 \sum_{v_1} \sum_{w_1} \exp(-\epsilon^0_{v_1}/k_B T) \times |\eta_1(v_1,w_1)|^2 \delta(\epsilon^0_{v_1} - \epsilon^0_{w_1} - \Delta E) \quad (59)$$

Thirdly, by adopting the harmonic approximation for the Fe motion we can also exploit a vast literature on multiphonon processes in other fields to evaluate the nuclear contribution to eq 59. Thus, if the single surviving nuclear mode is characterized by two harmonic potentials of frequency ω in both states ϕ_a and ϕ_b, for which the electronic energy gap is ΔE (<0), then the configurational change is specified by the reduced displacement as $\Delta = d(\mu_{NF}\omega/\hbar)^{1/2}$ where d is the coordinate distance between the minima of the two potential surfaces. The coupling strength of the mode is then $S = \Delta^2/2$ and the vibrational reorganization energy $E_r = S\hbar\omega$. The temperature dependence is reflected in the Bose occupation number $\bar{v} = [\exp(\hbar\omega/k_B T) - 1]^{-1}$, and the single-mode rate expression becomes[13]

$$W = A \exp[-S(2\bar{v} + 1) I_p\{2S\bar{v}(\bar{v} + 1)\}^{1/2}][(\bar{v} + 1)/\bar{v}]^{p/2} \quad (60)$$

where $A = 2\pi|V_{ab}|^2/\hbar^2\omega$, $p = |\Delta E|/\hbar\omega$ is the normalized energy gap, and $I_p(z)$ stands for the modified Bessel function of order p. Equation 60 is well-known in the theory of line shapes and of nonadiabatic solid-state processes. It exhibits a continuous transition from a low-temperature tunnelling expression

$$W = A \exp(-S) S^p/p! \qquad (k_B T \ll \hbar\omega) \quad (61)$$

determined by the low-temperature harmonic Poissonian overlap, to a high-temperature activated rate expression

$$W = A\hbar/(k_B T \hbar\omega S/\pi)^{1/2} \exp[-(S\hbar\omega + \Delta E)^2/4S\hbar\omega k_B T] \qquad (k_B T \gg \hbar\omega) \quad (62)$$

with a Gaussian-type activation energy $E_A = (S\hbar\omega + \Delta E)^2/4S\hbar\omega$. Although the appearance of eq 60 is thus formally identical with the result[13,30,39,40] for ET processes, this just reflects the common features of nonadiabatic processes in the harmonic approximation for the nuclear motion. However, as noted in section II, ET and AT processes display some important differences with respect to both the electronic coupling and the nuclear states.

In view of the large coordinate shift of the X_{HF} mode the harmonic approximation may seem inadequate for quantitative estimates of the parameters of the system. Thus, it was previously noted that anharmonicity in a single mode may modify both the absolute values of the calculated rate constants (by many orders of magnitude) and the qualitative appearance of the fundamental phenomenological kinetic laws, i.e., the Brønsted and the Arrhenius relationship.[43,50,51] For this reason, even though we shall generally apply the harmonic approximation, we also present a few calculations based on a representation of the X_{HF} mode by Morse potentials of the form

$$U_a(q_{HF}) = D[1 - \exp(-aq_{HF})]^2 \quad (63)$$

$$U_b(q_{HF}) = D\{1 - \exp[-a(q_{HF} - \Delta)]\}^2 + \Delta E \quad (64)$$

in the initial and in the final states. D is here the dissociation energy, a ($= (\hbar\omega/2D)^{1/2}$) is the anharmonicity constant, $q_{HF} = X_{HF}(\mu_{HF}\omega/\hbar)^{1/2}$, and Δ is the reduced displacement as previously defined. Our model calculations for the Morse potential are based on recasting eq 59 in the form

$$W \approx \frac{2\pi}{\hbar^2\omega} Z_1^{-1} |V_{ab}|^2 \sum_{v_1} \exp(-\epsilon^0_{v_1}/k_B T) |\eta_1(v_1,w_1)|^2 \quad (65)$$

$$(\epsilon_{w_1} = \epsilon_{v_1} + \Delta E)$$

where the Franck–Condon factors take the form[43,50]

$$\eta_1(v_1,w_1) = \left[\left(1 - \frac{2v_1}{p}\right)\left(1 - \frac{2w_1}{p}\right)\left(\frac{p}{v_1}\right)\left(\frac{p}{w_1}\right)\right]^{1/2} \times [\cosh(a/2)]^{-2p} \sum_{k=0}^{v} (-1)^{k+l} \frac{l!k!(p-1-k-l)!}{(p-1)!} \times \binom{p-w_1}{l}\binom{w_1}{l}\binom{p-v_1}{k}\binom{v_1}{k} [\tfrac{1}{2}(1 + e^{-a\Delta})]^k [1 + e^{-a\Delta})]^l \quad (66)$$

where $p = 2a^{-2} - 1$. We notice that the magnitude of $\eta_1(v_1,w_1)$ now also depends on the sign of the reduced displacement, as generally expected for asymmetric potentials. For exoergic processes negative values of Δ yield Franck–Condon factors which are larger than those for harmonic potentials. Such anharmonicity enhancement effects originate from a highly "stretched" nuclear mode in the final state. For positive Δ, opposite effects of anharmonicity retardation effects are expected.

Completion of our analysis would require that we consider the effects of "inhomogeneous broadening" (section II, point a). This effect originates from the spread of the energetic and structural parameters ΔE, $\hbar\omega$, and S which specify the two potential surfaces involved in the recombination process. The distribution of the barrier heights can be characterized by an empirical distribution function, which can be extracted numerically from the experimental (nonexponential) decay curves,[10] at least at high temperatures. In our present formalism we have assumed that the globular protein medium is weakly coupled to the reaction center and that the dominating accepting mode is the motion of Fe relative to the heme group (which is expected to be only weakly affected by the different conformational states). Accordingly, we assert that the major effect of inhomogeneous broadening involves the spread of the energy gap ΔE and we shall average the rate expressions, eq 59 and 60, over all values of ΔE but not over S. The concentration of the deoxy form at time t, $N(t)$, should then be written

$$N(t) = \int_0^\infty d|\Delta E| P(|\Delta E|) \exp[-W(S,|\Delta E|)t] \quad (67)$$

where $P(|\Delta E|)$ is the (normalized) probability, so that the reaction center in the individual conformational state would give rise to a recombination process characterized by a given value of $|\Delta E|$.

The two functions, $W(S,|\Delta E|)$ and $P(|\Delta E|)$, can in principle be separated.[10] Thus, inserting the high-temperature Arrhenius form, eq 62, in eq 67 and representing $N(t)$ em-

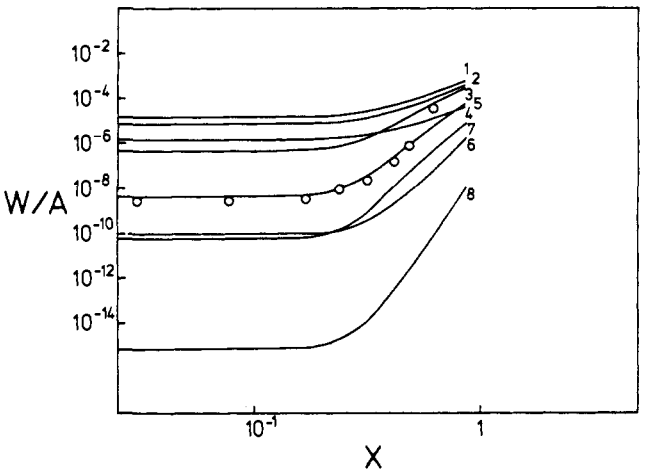

Figure 4. Model calculations of the temperature dependence of the Franck-Condon factors for nonadiabatic AT. The solid curves represent the theoretical plots of log (W/A) vs. $x = k_BT/\hbar\omega$, with $\hbar\omega = 100\ cm^{-1}$, for various S and p, calculated from eq 60. The numbers correspond to the following parameters: (1) $S = 60$, $p = 30$; (2) $S = 45$, $p = 20$; (3) $S = 20$, $p = 2$; (4) $S = 30$, $p = 8$; (5) $S = 25$, $p = 2$; (6) $S = 80$, $p = 30$; (7) $S = 30$, $p = 2$; (8) $S = 80$, $p = 20$. The circles represent the experimental values (ref 10) of log $(\tau_{0.75}^{-1})$ vs. log T with the limiting values at $T \to 0$ matched with curve 5 ($\tau_{0.75}^{-1} = 5\ s^{-1}$ for $T \to 0$).

pirically by a functional form which reproduces the experimental curves well ($N(t) = N(0)(1 + t/t_0)^{-n}$ where t_0 and n are empirical parameters[10]), $P(|\Delta E|)$ can be extracted from eq 67 and the high-temperature rate expression. Subsequently, by assuming that the same distribution over the conformational states prevails at low temperatures, the procedure can be inverted to calculate $W(|\Delta E|)$ numerically from the experimental low-temperature decay curves, $N(t)$, and the distribution function $P(|\Delta E|)$ estimated from the high-temperature data,[10] without invoking any particular model for the low-temperature process.

A disentanglement of eq 67 to provide W as a function of the barrier height in the low-temperature region without introducing additional models for the barrier itself was given explicitly for the β-Hb^{PMB}, i.e., a β-Hb subunit bound to paramercuribenzoate (PMB).[10c] This derivative differs from its parent compound by a stabilized high-spin "CO-free" state relative to the low-spin bound state. As a consequence, the peak barrier height for the recombination of CO with this compound is about twice as high as for β-Hb[10c] (0.088 vs. 0.045 eV), whereas the high-temperature preexponential factors are approximately equal (log A (s^{-1}) values are 9.2 and 9.4, respectively). The dynamics of the process contributing to the averaged Franck-Condon factors in the rate expression are in both cases primarily associated with the X_{HF} mode. The apparent temperature dependence for the resolved rate constants at different but fixed barrier heights (or $|\Delta E|$) referring to the Hb^{PMB}-CO process displays essentially the same features as the recombination between Hb and CO (apart from additive constants the experimental plots of log $k(E_A)$ vs. log T for the Hb^{PMB}-CO process and of log $(\tau_{0.75}^{-1})$ vs. log T for the Hb-CO process are in fact identical). Analysis of the data in terms of eq 60 also give almost the same physically plausible parameter values for the two cases. For these reasons, and in view of the narrow distribution functions calculated,[10] we shall advance an analysis of the Hb-CO system representing the rate constant in terms of $\tau_{0.75}^{-1}$. Such an analysis is expected to result in average (peak) values of the parameters S and p.

We now attempt to analyze the Hb-CO low-temperature ($T = 2$-100 K) recombination data[10] in terms of eq 60, which rests on the harmonic approximation. No reliable information regarding the energy gap ΔE for the Hb-CO recombination process is available at present. Austin et al.[10a] have estimated $\Delta E = -0.92$ eV for the Mb-CO system from the combination of thermodynamic data and of kinetic results. We have assumed that the Hb-CO recombination reaction is exoergic and viewed ΔE as a parameter, choosing the reasonable values $-\Delta E = 0.05$ to -0.5 eV (Table I). From the Arrhenius form of the high-temperature rate expression, eq 62, and the experimental activation energy (0.045 eV) we can subsequently find the corresponding values of $S\hbar\omega$ which are collected in Table I. This provides a sufficient basis for the model calculations of the Franck-Condon factors. In Figure 4 we portray the dependence of (W/A) on $k_BT/\hbar\omega$ according to eq 60 which were calculated for some reasonable values of the parameters S and p. These plots reveal the following features.

Table I. Nuclear and Electronic Parameters for the Dynamics of Hb-CO Recombination[a]

$-\Delta E$, eV	0.05	0.1	0.2	0.4	0.5
$S\hbar\omega$, eV	0.27	0.35	0.50	0.77	0.30
S	15-25	17-35	25-50	35-70	45-90
p	2-5	5-10	10-20	20-40	25-50
$\|\eta_1(0,p)\|^2$	10^{-9}-10^{-7}				10^{-6}-10^{-7}
V_{ab}, eV	10^{-5}-10^{-4}				10^{-6}-10^{-5}
V_{ab}, cm^{-1}	0.1-1				0.01-0.1

[a] The energy gap ΔE was introduced as a variable parameter which, together with the experimental high-temperature data, was utilized to estimate S. From the onset of the temperature dependence we estimate $\hbar\omega = 100\ cm^{-1}$. Finally, the electronic coupling V_{ab} was evaluated from the low-temperature experimental data.

(1) The curves display an "activationless" region at temperatures up to $k_BT/\hbar\omega \approx 0.1$-$0.2$. This region is followed relatively abruptly by a thermally activated region.

(2) The temperature dependence becomes more pronounced with increasing S at fixed p ($S > p$) and with decreasing p for a given value of S.

(3) The experimental transition region for the Hb-CO systems is 10-20 K, thus giving $\hbar\omega = 0.01$-0.02 eV or $\omega = 80$-$160\ cm^{-1}$. The resulting phonon coupling constant S and the value of $p = |\Delta E|/\hbar\omega$ are shown in Table I. This estimate of $\hbar\omega$ is not far from the values expected for the metal-ligand bending modes of heme complexes estimated from infrared spectroscopy[46] and from model calculations.[47]

(4) A cursory examination of the results of our model calculations, together with the experimental data,[10] which are portrayed in Figure 4, reveals that a reasonable reproduction of the experimental temperature dependence of the Hb-CO recombination reaction can be accomplished with the parameters $p = 2$-5 and $S = 20$-25. Taking $\hbar\omega \simeq 100\ cm^{-1}$ results in $\Delta E \simeq -0.05$ to -0.1 eV. This fit of the experimental data is not unique, as any set of S and p parameters, which are given in Table I, will result in a fair agreement with the experimental facts of life. For example, as is evident from Figure 4, the parameters $p = 40$-50 ($\Delta E = -0.5$ eV) together with $S = 80$-90 provide an adequate numerical fit of the experimental data. However, the large value of $S = 80$-90 together with $\hbar\omega = 100\ cm^{-1}$ implies a displacement of $d = 1$ Å in the equilibrium position of the Fe atom between the free and the bound states. This estimate for the value of d is too large. On the other hand, the value of $S = 20$-25 for the phonon coupling strength together with $\hbar\omega = 100\ cm^{-1}$ results in $d \simeq 0.4$-0.5 Å, which is consistent with the available structural data.[22-25] We thus conclude that the nuclear contribution to the Hb-CO recombination rate constant can be adequately described in terms of the parameters $p = 2$-5 ($\Delta E = -0.05$ to -0.1 eV), $S = 20$-25 ($d = 0.4$-0.5 Å), and $\hbar\omega \simeq 100\ cm^{-1}$. It should be pointed out, however, that the present analysis disregards the contribution of low-frequency medium modes and of the CO-histidine motion to the nuclear Franck-Condon factor, which is solely assigned to the configurational change in the

Fe-heme motion. Accordingly, the value of S as well as of Δ and of d, resulting from the simple present analysis, is somewhat overestimated. The value of d (obtained at a fixed value of ΔE) should be viewed as an upper limit for the actual displacement of the Fe atom outside the heme plane. Accordingly, the value of $|\Delta E| = +0.05$ to $+0.1$ eV estimated for the "best fit" of the structural data constitutes a lower limit for the actual absolute value of the energy gap. A more refined analysis, which will go beyond the one-dimensional motion prescribed by eq 59 and 60, will result in higher values of $|\Delta E|$ while d will remain in the physically acceptable range of 0.4-0.5 Å.

(5) From the "best" values of the parameters p and S we can estimate the low-temperature Franck-Condon factor $|\eta_1(0,p)|^2 = 10^{-7}$-$10^{-9}$. Utilizing the low-temperature experimental result $W(T \to 0) = 5\ s^{-1}$, we can provide an estimate of the electronic coupling term V_{ab}, which is presented in Table I. The value $V_{ab} = 0.1$-$1\ cm^{-1}$ resulting from the analysis of the kinetic data is in good agreement with our rough estimate $V_{ab} \approx 1\ cm^{-1}$ (see section II) for the second-order spin-orbit coupling.

This low value of V_{ab} justifies the use of the nonadiabatic approach for Hb-CO recombination reactions. The validity condition for this approach, as expressed in terms of the semiclassical Landau-Zener formalism, is[52,53]

$$2\pi|V_{ab}|^2/\hbar v|\Delta F| \ll 1 \tag{68}$$

where ΔF is the difference between the slope of the zero-order potential surface at the intersection point and v is the velocity with which the system passes this intersection point. Inserting the thermal velocity $(2k_BT/\mu_{HF})^{1/2}$ the validity condition, eq 68, takes the form

$$\kappa = 2\pi|V_{ab}|^2/(\hbar^3\omega^3 k_B TS)^{1/2} \ll 1 \tag{69}$$

For the parameter values of Table I, we get

$$\kappa = 10^{-5}\text{-}10^{-7} \tag{70}$$

providing an adequate justification for the applicability of the nonadiabatic formalism.

A similar analysis of the experimental results can be carried out going beyond the harmonic approximation for the X_{HF} mode. We have performed few calculations using the rate expression, eq 65, with Franck-Condon factors for Morse potentials, eq 66, which are available in a relatively compact form.[50] These results are presented only for the sake of comparison since, in addition to introducing still another parameter, the calculations performed using Morse potentials cannot be conducted in a consistent fashion. The small vibrational frequency value appropriate for the Hb-CO system, together with any reasonable values of the anharmonicity constant a, would result in too low values of the dissociation energy of the iron-heme bond (0.3-1 eV). However, for sufficiently small ΔE this difficulty can be ignored in the present discussion. Since the Franck-Condon factors for Morse potentials with a negative coordinate displacement are larger than for harmonic potentials, the application of the Morse potentials will then modify the previous conclusions primarily in either of two ways: (a) The electronic integral will be smaller than the value estimated on the basis of harmonic potentials for the nuclear contribution. Thus, using the values of $\hbar\omega = 100\ cm^{-1}$, $\Delta E = -0.05$ eV, and $\Delta = -5$ to -7, the resulting Franck-Condon factors for Morse potentials (with $a = 0.15$) are 3×10^{-2} and 10^{-3} for $\Delta = -5$ and for $\Delta = -7$, respectively, which considerably exceed the Franck-Condon factors based on the harmonic model. (b) Larger displacement values, $|\Delta|$, than those obtained from the harmonic approximation are now required for a reasonable fit of the experimental results. Thus, Δ values of about -10 and $\hbar\omega \approx 100\ cm^{-1}$ can reproduce the experimental data and, furthermore, provide reasonable values of the electronic coupling term, $V_{ab} \approx 0.1$-$1\ cm^{-1}$. This would give a shift distance for the Fe atom of 0.75 Å, which coincides with the value reported by Perutz[20] but which now is generally believed to be too high.[21,44,47]

V. Relation of Multiphonon Theory to Gamov Tunnelling

The low-temperature rate constant for nonadiabatic multiphonon AT or ET processes considered in the present and in previous work[13,30] represents in both cases nuclear tunnelling between two bound vibrational manifolds. In the single-mode harmonic approximation the resulting low-temperature expression is $W = AF$, where the Franck-Condon factor $F = \exp(-S)S^p/p!$ (eq 61). On the other hand, the nuclear tunnelling effect for AT processes is commonly described by means of the Gamov tunnelling formula[7,10,54,55] for the tunnelling probability so that

$$W = \nu_0 \exp\{-\gamma d(\mu E_A)^{1/2}/\hbar\} \tag{71}$$

where ν_0 is a characteristic frequency with which a particle of nuclear mass μ hits a barrier of height E_A and width d. γ is a numerical factor which depends on the shape of the barrier. For a parabolic barrier γ is $\pi/\sqrt{2}$ and for a square barrier it is $2\sqrt{2}$. We shall provide here some justification for the use of this functional form for nonadiabatic AT by showing that the exponential term in the Gamov equation is equivalent to the nuclear vibrational overlap factors.

For larger values of p, which are appropriate in the present context, insertion of Stirling's approximation $p! = \exp[p(\ln p - 1)]$ in eq 61 gives

$$W = A\exp(-S)\exp(-\gamma p);\ \gamma = \ln(p/S) - 1;\quad A = 2\pi|V_{ab}|^2/\hbar^2\omega \tag{72}$$

This can be recast in the form

$$W = A\exp[-(S\hbar\omega - |\Delta E|)/\hbar\omega] \times \exp[-(1+\gamma)(|\Delta E|)/\hbar\omega] \tag{73}$$

Introducing the relations $E_A = (S\hbar\omega - |\Delta E|)^2/2S\hbar\omega$ and $\Delta^2 = d^2(\mu\omega/\hbar)$, eq 73 can be rewritten as

$$W = A\exp[-\sqrt{2}d(\mu E_A)^{1/2}/\hbar]\exp[-(1+\gamma)(|\Delta E|/\hbar\omega] \tag{74}$$

The second exponent in eq 74 is of minor importance since $1 + \gamma$ is a negative quantity, the numerical value of which in the present case is 3-4, but generally smaller the closer p is to S. Thus eq 74 bears a close formal analogy to the Gamov formula, eq 71. However, the preexponential factor, ν_0, in the heuristic expression, eq 71, is now different. This simple analysis shows the following.

(1) The low temperature rate constant for AT can be recast in terms of a product $W = AF$, of a nuclear contribution F and an electronic contribution A, according to eq 61.

(2) Equation 74 establishes the equivalence between the nuclear contribution to the AT rate constant and a tunnelling formula. The Franck-Condon nuclear overlap factor, F, for exoergic processes can be recast in a form very close to the Gamov formula. This result is useful but not surprising as it just shows that the WKB approximation (and the representation of the nuclear wave functions by the quasi-classical approximation[56]) is applicable for the calculation of Franck-Condon factors both between two bound states and between a bound and a continuum state as for the original Gamov tunnelling.[57]

(3) The preexponential electronic factor A in the exoergic rate expression, eq 74, cannot be expressed in terms of Gamov's preexponential factor ν_0 of eq 71. Rather, the multiphonon expression $A = 2\pi|V_{ab}|^2/\hbar^2\omega$ has to be utilized for the preexponential factor.

(4) Equation 74 provides an interesting alternative expres-

sion for an energy gap law (EGL) for exoergic processes. The common EGL for multiphonon processes relates the low-temperature rate to the energy gap ΔE in the form $\ln W = \text{const} - \gamma(\Delta E/\hbar\omega)$, as is evident for eq 72. Equation 74 provides a useful relation between the low-temperature rate and the activation energy E_A in the approximate form $\ln W = \text{const}' - \alpha(E_A)^{1/2}$ with $\alpha = \sqrt{2}d\mu^{1/2}/\hbar$.

(5) For quantitative analysis of low-temperature AT data the fully fledged multiphonon rate expression has to be utilized.

VI. Concluding Remarks

The purpose of this work is to provide a theoretical scheme for the description of nonadiabatic multiphonon AT processes involving two well-defined electronic states and to apply this scheme to an analysis of the interesting and important recombination process[10] between Hb and CO, for which many of the basic assumptions of the theory seem to be valid. We should note, however, that nonadiabaticity in AT processes is likely to be the exception rather than the rule. Thus, apart from the Hb–CO recombination and related processes, nearly all other AT processes are likely to proceed on a single potential surface and therefore correspond to the opposite limit of adiabatic AT processes. Typical adiabatic AT processes involve ligand substitution[58] and other heavy atom group transfer,[59] configurational and interstitial relaxation and diffusion of ions in insulating solids,[60] the diffusion of hydrogen atoms in metals,[61] tunnelling between low-frequency phonon states which determines anomalous heat capacity and ultrasonic attenuation effects in amorphous solids,[62] tunnelling in molecules[63] (e.g., the ammonia inversion), and nuclear tunnelling between chiral isomers.[64] Most previous attempts to formulate a theory for adiabatic AT rest on a nuclear adiabatic approximation and semiclassical rate theory. The development of a quantum mechanical theory for this class of adiabatic processes would constitute a challenging theoretical goal, being of considerable interest in the context of a variety of chemical, physical, and biological phenomena.

Acknowledgments. The authors would like to express their gratitude to Professor Hans Frauenfelder, University of Illinois, Urbana, Ill., for drawing our attention to the interesting field of the hemoglobin and myoglobin recombination processes and for many stimulating discussions. We would also like to thank Professor P. J. Stephens, University of Southern California, for useful information about recent data on the electronic structure of these compounds.

References and Notes

(1) (a) Tel-Aviv University; (b) The Technical University of Denmark.
(2) (a) D. DeVault and B. Chance, *Biophys. J.*, **6**, 825 (1966); (b) P. L. Dutton, K. J. Kaufmann, B. Chance, and P. M. Rentzepis, *FEBS Lett.*, **60**, 275 (1975).
(3) K. Peters, P. Avouris, and P. M. Rentzepis, *Biophys. J.*, **23**, 207 (1978).
(4) B. Chance, D. DeVault, V. Legallais, L. Mela, and T. Yonetani in "Fast Reactions and Primary Processes in Chemical Kinetics", S. Claesson, Ed., Interscience, New York, 1967, pp 457–468.
(5) D. H. Blow, *Acc. Chem. Res.*, **9**, 145 (1976).
(6) M. W. Hunkapillar, M. D. Forgac, and J. H. Richards, *Biochemistry*, **15**, 5581 (1976).
(7) K. Peters, M. L. Applebury, and P. M. Rentzepis, *Proc. Natl. Acad. Sci. U.S.A.*, **74**, 3119 (1977).
(8) (a) J. H. Wang, *Science*, **161**, 328 (1968); (b) *Proc. Natl. Acad. Sci. U.S.A.*, **66**, 874 (1970).
(9) M. L. Ludwig and W. N. Lipscomb in "Inorganic Biochemistry", Vol. 1, G. I. Eichhorn, Ed., Elsevier, Amsterdam, 1973, pp 438–482, and other chapters in this volume.
(10) (a) R. H. Austin, K. W. Beeson, L. Eisenstein, H. Frauenfelder, and I. C. Gunsalus, *Biochemistry*, **14**, 5355 (1975); (b) N. Alberding, R. H. Austin, K. W. Beeson, S. S. Chan, L. Eisenstein, H. Frauenfelder, and T. M. Nordlund, *Science*, **192**, 1002 (1976); (c) N. Alberding, S. S. Chan, L. Eisenstein, H. Frauenfelder, D. Good, I. C. Gunsalus, T. M. Nordlund, M. F. Perutz, A. H. Reynolds, and L. B. Sorensen, *Biochemistry*, **17**, 43 (1978).
(11) H. C. Longuet-Higgins and P. W. Higgs, *Nature (London)*, **173**, 809 (1954).
(12) J. J. Hopfield, *Proc. Natl. Acad. Sci. U.S.A.*, **71**, 3640 (1974).
(13) J. Jortner, *J. Chem. Phys.*, **64**, 4860 (1976).
(14) A. M. Kuznetsov, N. C. Søndergård, and J. Ulstrup, *Chem. Phys.*, **29**, 383 (1978).
(15) R. R. Dogonadze, Yu. I. Kharkats, and J. Ulstrup, *J. Theor. Biol.*, **40**, 259 (1973).
(16) R. R. Dogonadze, A. M. Kuznetsov, and J. Ulstrup, *J. Theor. Biol.*, **69**, 239 (1977).
(17) R. R. Dogonadze and A. M. Kuznetsov, *Prog. Surf. Sci.*, **6**, 1 (1975).
(18) R. R. Dogonadze and A. M. Kuznetsov, "Physical Chemistry. Kinetics", Viniti, Moscow, 1973.
(19) R. R. Dogonadze, A. M. Kuznetsov, and M. A. Vorotyntsev, *Dokl. Akad. Nauk SSSR, Ser. Fiz. Khim.*, **209**, 1135 (1973).
(20) W. Bolton and M. F. Perutz, *Nature (London)*, **228**, 551 (1970).
(21) M. F. Perutz, E. J. Reidner, J. E. Ladner, J. G. Boetlestone, C. Ho, and E. F. Slade, *Biochemistry*, **13**, 2187 (1974).
(22) H. C. Watson, *Prog. Stereochem.*, **4**, 299 (1968).
(23) J. C. Norvell, A. C. Nunes, and B. P. Schoenborn, *Science*, **190**, 568 (1975).
(24) T. Tanako, quoted in ref 47.
(25) J. L. Hoard and W. R. Scheidt, *Proc. Natl. Acad. Sci. USA*, **70**, 3919 (1973).
(26) (a) S.-M. Peng and J. A. Ibers, *Science*, **140**, 568 (1975); (b) S.-M. Peng and J. A. Ibers, *J. Am. Chem. Soc.*, **98**, 8032 (1976).
(27) J. M. Rifkind in "Inorganic Biochemistry", Vol. 2, G. I. Eichhorn, Ed., Elsevier, Amsterdam, 1973, pp 832–891.
(28) (a) D. A. Case, B. H. Huynk, and M. Karplus, *J. Am. Chem. Soc.*, submitted; (b) M. Zermer, M. Gouterman, and H. Kobayashi, *Theor. Chim. Acta*, **6**, 363 (1966); (c) A. K. Chung and M. W. Makinen, *J. Chem. Phys.*, **68**, 1913 (1978).
(29) (a) R. Englman and J. Jortner, *Mol. Phys.*, **18**, 145 (1970); (b) K. F. Freed and J. Jortner, *J. Chem. Phys.*, **52**, 6272 (1970); (c) R. R. Dogonadze, A. M. Kuznetsov, and M. A. Vorotyntsev, *Phys. Status Solidi B*, **54**, 125 (1972).
(30) N. R. Kestner, J. Logan, and J. Jortner, *J. Phys. Chem.*, **78**, 2148 (1974).
(31) V. G. Levich, R. R. Dogonadze, and A. M. Kuznetsov, *Electrochim. Acta*, **13**, 1025 (1968).
(32) V. G. Levich, R. R. Dogonadze, E. D. German, A. M. Kuznetsov, and Yu. I. Kharkats, *Electrochim. Acta*, **15**, 353 (1970).
(33) T. Holstein, *Ann. Phys.*, **8**, 343 (1959).
(34) M. L. Goldberger and K. M. Watson, "Collision Theory", Wiley, New York, 1964.
(35) H. C. Longuet-Higgins, *Adv. Spectrosc.* **2**, 429 (1961).
(36) A. Nitzan and J. Jortner, *J. Chem. Phys.*, **56**, 3360 (1972).
(37) R. Kobo and Y. Toyozawa, *Prog. Theor. Phys.*, **13**, 161 (1955).
(38) R. R. Dogonadze and Z. D. Urushadze, *J. Electroanal. Chem.*, **32**, 235 (1971).
(39) R. A. Marcus, *J. Chem. Phys.*, **24**, 966 (1956).
(40) V. G. Levich and R. R. Dogonadze, *Collect. Czech. Chem. Commun.*, **26**, 193 (1961).
(41) R. R. Dogonadze, A. M. Kuznetsov, M. A. Vorotyntsev, and M. G. Zakaraya, *J. Electroanal. Chem.*, **75**, 315 (1977).
(42) (a) J. S. Griffith, "The Theory of Transition Metal Ions", Cambridge University Press, New York, 1961; C. J. Ballhausen, "Introduction to Ligand Field Theory", McGraw-Hill, New York, 1962.
(43) M. D. Sturge, *Phys. Rev. B*, **8**, 6 (1973).
(44) O. Lumpkin and W. T. Dixon, *J. Chem. Phys.*, **68**, 3485 (1978).
(45) W. A. Eaton, L. K. Hanson, P. J. Stephens, J. O. Sutherland, and J. B. R. Dunn, *J. Am. Chem. Soc.*, **100**, 4991 (1978).
(46) L. Boucher and J. J. Katz, *J. Am. Chem. Soc.*, **89**, 1340 (1967).
(47) B. D. Olafson and W. A. Goddard III, *Proc. Natl. Acad. Sci. U.S.A.*, **74**, 1315 (1977).
(48) A. Nitzan and J. Jortner, *Theor. Chim. Acta*, in press.
(49) T. Holstein, *Philos. Mag.*, **37**, 499 (1978).
(50) (a) N. C. Søndergård, J. Ulstrup, and J. Jortner, *Chem. Phys.*, **17**, 417 (1976); (b) P. A. Fraser and W. R. Jarmain, *Proc. Phys. Soc., London, Sect. A*, **66**, 1153 (1953).
(51) N. Brüniche-Olsen and J. Ulstrup, *J. Chem. Soc., Faraday Trans. 2*, **74**, 1690 (1978).
(52) C. Zener, *Proc. R. Soc. London, Ser. A*, **137**, 696 (1932).
(53) R. R. Dogonadze and A. M. Kuznetsov, *Teor. Eksp. Khim.*, **6**, 298 (1970).
(54) V. I. Gol'danskij, *Annu. Rev. Phys. Chem.*, **27**, 85 (1976).
(55) R. P. Bell, "The Proton in Chemistry", 2nd ed., Chapman and Hall, London, 1973.
(56) L. D. Landau and E. M. Lifshitz, "Quantum Mechanics", 2nd ed., Pergamon Press, Oxford, 1965.
(57) G. Ganov, *Z. Phys.*, **51**, 204 (1928).
(58) H. Taube, "Electron Transfer Reactions in Solution", Academic Press, New York, 1970.
(59) E. D. German and R. R. Dogonadze, *Int. J. Chem. Kinet.*, **6**, 457, 467 (1974).
(60) K. F. Freed and F. K. Fong, *J. Chem. Phys.*, **63**, 2890 (1975).
(61) C. P. Flynn and A. M. Stoneham, *Phys. Rev. B*, **1**, 3966 (1970).
(62) (a) P. W. Anderson, B. I. Halparin, and C. M. Varma, *Philos. Mag.*, **25**, 1 (1972); (b) J. Jäckle, *Z. Phys.*, **257**, 212 (1972); (c) W. A. Phillips, *J. Low Temp. Phys.*, **7**, 331 (1972).
(63) M. D. Harmony, *Chem. Soc. Rev.*, **1**, 211 (1972).
(64) L. Rosenfeld, *Z. Phys.*, **52**, 161 (1929).